

Conf-841201--26

Consolidated Fuel Reprocessing Program

CONF-841201--26

PERFORMANCE CHARACTERISTICS OF AXISYMMETRIC
VENTURI-LIKE REVERSE-FLOW DIVERTERS

DE85 005276

G. V. Smith*
Mechanical & Aerospace Engineering Department
University of Tennessee
Knoxville, Tennessee 37996

and

R. M. Counce
Fuel Recycle Division
Oak Ridge National Laboratory†
Oak Ridge, Tennessee 37831

Summary of paper for presentation
at the
American Society of Mechanical Engineers
Winter Annual Meeting

December 9-14, 1984

New Orleans, Louisiana

By acceptance of this article, the
publisher or recipient acknowledges
the U.S. Government's right to
retain a nonexclusive, royalty-free
license in and to any copyright
covering the article.

DISCLAIMER

This report was prepared as an account of work sponsored by an agency of the United States Government. Neither the United States Government nor any agency thereof, nor any of their employees, makes any warranty, express or implied, or assumes any legal liability or responsibility for the accuracy, completeness, or usefulness of any information, apparatus, product, or process disclosed, or represents that its use would not infringe privately owned rights. Reference herein to any specific commercial product, process, or service by trade name, trademark, manufacturer, or otherwise does not necessarily constitute or imply its endorsement, recommendation, or favoring by the United States Government or any agency thereof. The views and opinions of authors expressed herein do not necessarily state or reflect those of the United States Government or any agency thereof.

*Address correspondence to Gary V. Smith, Mechanical & Aerospace Engineering Department, University of Tennessee, Knoxville, Tennessee 37996-2210.

†Operated by Martin Marietta Energy Systems, Inc., for the U.S. Department of Energy.

MASTER

Consolidated Fuel Reprocessing Program

PERFORMANCE CHARACTERISTICS OF AXISYMMETRIC
VENTURI-LIKE REVERSE-FLOW DIVERTERS*

G. V. Smith
Mechanical and Aerospace Engineering Department
University of Tennessee
Knoxville, Tennessee 37996

and

R. M. Counce
Fuel Recycle Division
Oak Ridge National Laboratory
Oak Ridge, Tennessee 37831

ABSTRACT

This paper presents experimental and model-predicted pressure-flow characteristics of axisymmetric venturi-like reverse-flow diverters (RFDs), the key component of fluid pumping systems utilized for the transport of hazardous fluids. The effects of several key geometric parameters, operating conditions, and fluid properties on the performance of the RFD are presented and compared to model predictions. The results indicate good agreement between data and theory over a large portion of the range of variables studied. Cavitation is observed to be the primary factor in limiting the performance of the RFD at small values of load impedances.

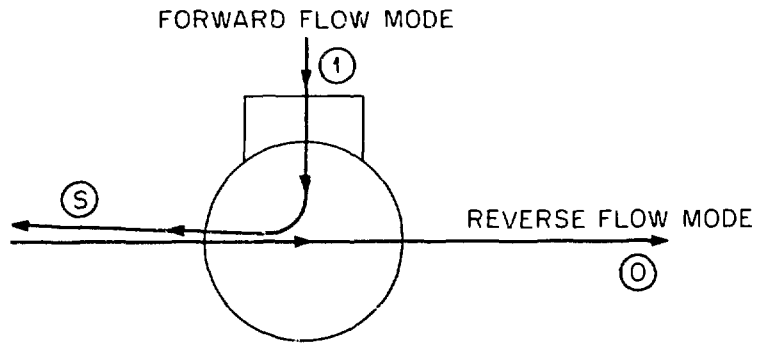
*Research sponsored by the Office of Spent Fuel Management and Reprocessing Systems, U.S. Department of Energy, under Contract No. DE-AC05-84OR21400 with Martin Marietta Energy Systems, Inc.

1. INTRODUCTION

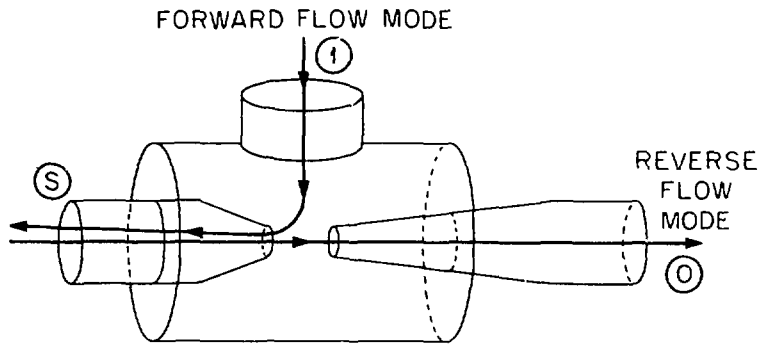
This paper presents experimental and model-predicted pressure-flow characteristics for axisymmetric RFDs. An RFD, shown schematically in Fig. 1a, is a three-port device with two modes of flow — a forward mode from port 1 to port *i* and a reverse mode from port *i* to port 0. Such devices are important components of air-motivated pumping systems which rely on manipulation of fluid dynamic properties to eliminate moving parts. Such pumping systems have been used extensively in British nuclear fuel reprocessing facilities¹⁻⁷, and it is anticipated that these pumping systems will prove to be extremely useful in harsh chemical process environments where ultrareliable leak-free operation is required.¹

The venturi-like RFD is shown schematically in Fig. 1b. In the reverse-flow direction, the increased momentum flux of the fluid emanating from the nozzle transports the fluid across the gap separating the nozzle from the receiver/diffuser. The fluid entering the receiver is decelerated in the diffuser, resulting in a portion of the dynamic pressure of the fluid being converted to static pressure at the diffuser outlet. In the forward-flow direction, the fluid does not flow appreciably to port 0 because of a sufficiently large load impedance, such as a large hydrostatic head.

Although some performance data have been reported on planar RFDs⁸, this study presents a rather extensive investigation of the diffuser size, gap between nozzle and receiver, supply pressure, and fluid properties on the overall performance of the RFD.



(a) GENERAL RFD



(b) VENTURI-RFD

Fig. 1. Schematic of reverse flow diverter.

The three RFDs utilized in this study were machined out of Plexiglas and had nozzle exit and receiver inlet diameters of 0.94, 1.32, and 1.84 cm. In one series of tests, a receiver/diffuser with a constant area developing section (~10 cm in length) preceding the diffuser was used. The design of the diffusers was such that separation of the flow would not be normally expected, as suggested by the stability map of Fox and Kline.⁹

Input and output pressures were measured with pressure sensor/transmitters. Flow rates were computed from level changes in tanks associated with fluid movements. The experimental system features an automatic data acquisition system controlled by a Bristol UCS unit processor controller.

2. MATHEMATICAL MODELS

The development of the mathematical models presented in this section are predicated on the assumption of the flow in the RFD being incompressible and steady. It is also assumed that the static pressure in the volume surrounding the nozzle and the receiver/diffuser (i.e., the plenum) is constant at some known value imposed, perhaps by a hydrostatic head. Pressures will be normalized with respect to the pressure drop across the nozzle; flow rates will be normalized with respect to the flow rate through the nozzle; velocities will be normalized with respect to the ideal velocity exiting the nozzle; and areas will be normalized with respect to the nozzle exit area.

2.1 Nozzle Model

The basic equation for the nozzle flow is Bernoulli's equation, which was written for the region between the nozzle inlet where the velocity is small and the nozzle exit where the pressure is equal to the imposed plenum pressure. This equation for the nozzle exit velocity, coupled with the exit nozzle area and an equation of continuity, yields for the input flow

$$Q_i = C_d A_n \sqrt{2(P_i - P_l)/\rho} \quad , \quad (1)$$

where a discharge coefficient has been added to account for losses in the nozzle.

2.2 Receiver/Diffuser - Source Flow Model

The modeling of the flow through the receiver/diffuser is probably the key to an accurate description of the pressure-flow characteristics of the RFD. One technique that has achieved some success in modeling the flow through a receiver/diffuser in a fluid amplifier¹⁰ is to consider the flow at the receiver inlet as a "source" or "driving" pressure equal to the sum of the static and dynamic pressures of the jet. The difference between this source or total pressure of the jet and the total pressure at the diffuser outlet is equal to the losses occurring within the receiver/diffuser. This may be expressed as

$$P_s - (P_o + 1/2\rho Q_o^2/A_o^2) = K_d 1/2\rho Q_o^2/A_r^2 \quad , \quad (2)$$

where the diffuser loss coefficient is based on the maximum velocity occurring within the receiver/diffuser.

This source or total pressure of the jet emanating from the nozzle of the RFD is noted to be equal to the supply pressure applied to the

nozzle inlet minus the pressure drop due to irreversibilities in the flow through the nozzle.

In Eq. (2), the diffuser loss coefficient may be replaced by the more frequently utilized pressure recovery coefficient defined as the fraction of dynamic pressure entering a diffuser which is converted to static pressure at the diffuser outlet. Mathematically, these two quantities are related by

$$K_d = 1 - C_p - (A_r/A_o)^2 . \quad (3)$$

Substitution of Eq. (3) into Eq. (2) yields

$$P_s - P_o = (1 - C_p) 1/2\rho Q_o^2/A_r^2 . \quad (4)$$

Since the source pressure may be expressed as

$$P_s = P_i - 1/2\rho [(1 - C_d^2)/C_d^2] Q_i^2/A_n^2 , \quad (5)$$

use of this expression to eliminate the source pressure in Eq. (4)

yields

$$\bar{P}_i - \bar{P}_o = 1/2\rho [(1 - C_p) Q_o^2/A_r^2 + \frac{1 - C_d^2}{C_d^2} Q_i^2/A_n^2] . \quad (6)$$

Normalization of Eq. (6) through use of Eq. (1) yields

$$P_o - P_i = C_d^2 [1 - (1 - C_p) \bar{Q}_o^2/\bar{A}_r^2] . \quad (7)$$

2.3 Receiver/Diffuser - Inviscid Jet Model

A different approach to a mathematical model of the pressure-flow characteristics of the receiver/diffuser is to consider the jet incident on the receiver inlet as an inviscid jet. To simplify this analysis, the assumptions are made that the cross sectional area of the jet in the plenum region is equal to the receiver inlet area and that the flow in the nozzle of the RFD is ideal.

The cross sectional area of the jet stream tube in the immediate vicinity of the receiver inlet is determined by the static pressure in

this region. If the static pressure in the receiver inlet is less than the ambient (plenum) pressure, the fluid is accelerated as it enters the receiver, resulting in a reduction in cross sectional area of the jet as shown schematically in Fig. 2a. Because of this pressure gradient now existing between the ambient fluid and the receiver inlet, additional fluid is induced into the receiver through the area created by the acceleration of the jet. It is assumed that this flow is mixed in the receiver region, which results in a uniform velocity profile entering the diffuser.

If the pressure in the receiver inlet is greater than ambient pressure, the jet is decelerated, resulting in an increase in the stream tube area as shown schematically in Fig. 2b. Under these conditions only a portion of the jet enters the receiver with an assumed uniform velocity profile which remains unchanged in the receiver region.

Bernoulli's equation written for the jet between section 1, the plenum region, and section 2, the receiver inlet, may be expressed in nondimensional form as

$$\bar{V}_{j_2}^2 = 1 + \bar{P}_1 - \bar{P}_2 . \quad (8)$$

Since continuity states that

$$\bar{A}_{j_2} \bar{V}_{j_2} = \bar{A}_{j_1} \bar{V}_{j_1} = 1 , \quad (9)$$

the jet cross sectional area at the receiver entrance is

$$\bar{A}_{j_2} = 1/\bar{V}_{j_2} = [1 + \bar{P}_1 - \bar{P}_2]^{-1/2} . \quad (10)$$

Considering first the flow characteristics when the pressure in the receiver inlet is less than the ambient pressure, the portion of the receiver inlet area through which induced fluid flows is given by

$$\bar{A}_{in_2} = 1 - \bar{A}_{j_2} . \quad (11)$$

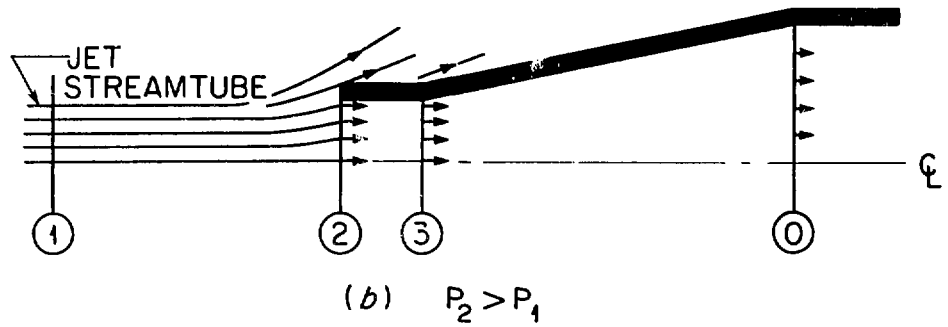
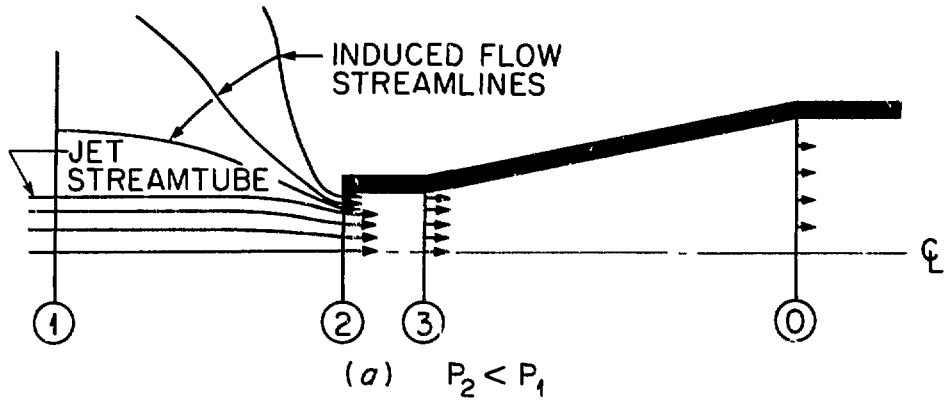


Fig. 2. Inviscid jet and receiver diffuser interaction.

Applying Bernoulli's equation between the receiver inlet, where the velocity is small, the plenum region, where the pressure is reduced, yields for the normalized square of the velocity of the induced flow in the receiver inlet as

$$\bar{V}_{in_2}^2 = \bar{P}_1 - \bar{P}_2 \quad (12)$$

The induced flow through the receiver inlet is therefore

$$\bar{Q}_{in_2} = \bar{A}_{in_2} \bar{V}_{in_2} = [1 - \bar{A}_{j_2}] \sqrt{\bar{P}_1 - \bar{P}_2} \quad (13)$$

Continuity yields for the total flow through the receiver, and also the diffuser, as

$$\bar{Q}_o = 1 + \bar{Q}_{in_2} \quad (14)$$

Substitution of Eqs. (10) and (13) into Eq. (14) yields

$$\bar{Q}_o = 1 + [1 - (1 + \bar{P}_1 - \bar{P}_2)^{-1/2}] \sqrt{\bar{P}_1 - \bar{P}_2} \quad (15)$$

It is assumed that the nonuniform velocity profile at section 2 is mixed in the receiver region, yielding a uniform velocity profile at section 3. The pressure at section 3 is determined from the momentum equation in normalized form as

$$\bar{P}_2 - \bar{P}_3 = 2[\bar{V}_3^2 - \bar{A}_{j_2} \bar{V}_{j_2}^2 - \bar{A}_{in_2} \bar{V}_{in_2}^2] \quad (16)$$

Substitution of Eqs. (8), (11), (12), and (16), along with continuity at section 3 and $\bar{Q}_o = \bar{V}_3$ yields

$$\bar{P}_3 - \bar{P}_1 = \bar{P}_1 - \bar{P}_2 + 2(1 + \bar{P}_1 - \bar{P}_2)^{-1/2} - 2\bar{Q}_o^2 \quad (17)$$

The definition of the pressure recovery coefficient,

$$C_p = \frac{P_0 - P_3}{1/2\rho V_3^2} = (\bar{P}_0 - \bar{P}_3)/\bar{Q}_o^2, \quad (18)$$

is utilized to determine the output pressure from the pressure at the diffuser inlet. Combining Eqs. (17) and (18) gives

$$\bar{P}_0 - \bar{P}_1 = \bar{P}_1 - \bar{P}_2 + 2(1 + \bar{P}_1 - \bar{P}_2)^{-1/2} - (2 - C_p)\bar{Q}_o^2 \quad (19)$$

For the case of $P_2 < P_1$, Eqs. (15) and (19) are two equations in three unknowns, $\bar{P}_0 - \bar{P}_1$, \bar{Q}_0 , and $\bar{P}_1 - \bar{P}_2$. Since it is desired to know \bar{Q}_0 as a function of $\bar{P}_0 - \bar{P}_1$, the unknown $\bar{P}_1 - \bar{P}_2$ could conceivably be eliminated between these two equations; however, the resulting complex algebraic equation suggests that it is more useful to leave the equations separate.

For the condition where the receiver inlet pressure is greater than the plenum pressure, the flow rate in the receiver is equal to that portion of the jet "captured" by the receiver

$$\bar{Q}_0 = \bar{V}_{j_2} = (1 + \bar{P}_1 - \bar{P}_2)^{1/2} . \quad (20)$$

Since $V_{j_2} = V_3$, the pressure at section 2 is equal to the pressure at section 3. The expression for the pressure recovery coefficient may therefore be expressed as

$$\bar{P}_0 - \bar{P}_1 = \bar{P}_2 - \bar{P}_1 + C_p \bar{Q}_0^2 . \quad (21)$$

Combining Eqs. (20) and (21) yields

$$\bar{P}_0 - \bar{P}_1 = 1 - (1 - C_p) \bar{Q}_0^2 . \quad (22)$$

It should be noted that Eq. (7) becomes identical to Eq. (22) if the assumptions of inviscid nozzle flow and equal nozzle exit and receiver inlet area are made. For the condition of $P_2 > P_1$, the receiver area is subjected to a uniform jet velocity profile which is equivalent to the previous assumption of a source flow model.

3. DISCUSSION OF RESULTS

The steady-state characteristics of the RFD are presented and, where applicable, compared to the mathematical models developed. The effects of various parameters such as supply pressure, nozzle and receiver areas, gap ratio (nozzle-receiver separation distance divided

by nozzle diameter), and fluid property variation are presented and discussed. All data presented are for water at ambient conditions as the working fluid except for those cases distinctly noted.

3.1 Input Characteristics

The input characteristics are presented in the format of the measured flow rate through the nozzle of the RFD divided by the nozzle exit area, plotted versus the pressure drop across the nozzle as indicated by Fig. 3. As expected, this format collapses the data for water into, essentially, a single curve and agrees quite well with the predicted characteristics for a discharge coefficient of unity. This figure demonstrates the validity of the assumption that the flow through the nozzle, for water at least, may be approximated as ideal. It is obvious, however, that as the fluid viscosity increases, the deviation of the characteristics from ideal will increase. This is evident by the data in this figure for the 40 wt % sucrose solution with a kinematic viscosity of $6 \text{ m}^2/\text{s}$, which indicates a slight reduction in flow due to increased viscous losses.

3.2 Output Characteristics

Figures 4, 5, and 6 present the output characteristics as the normalized output flow rate versus the normalized static pressure rise across the receiver/diffuser for nozzle diameters of 0.94, 1.32, and 1.85 cm respectively. Each figure is for a gap ratio of unity and also presents the predicted characteristics from the two mathematical models. As the models predict, the data for different supply or input pressures tend to collapse into a single curve especially for higher output load

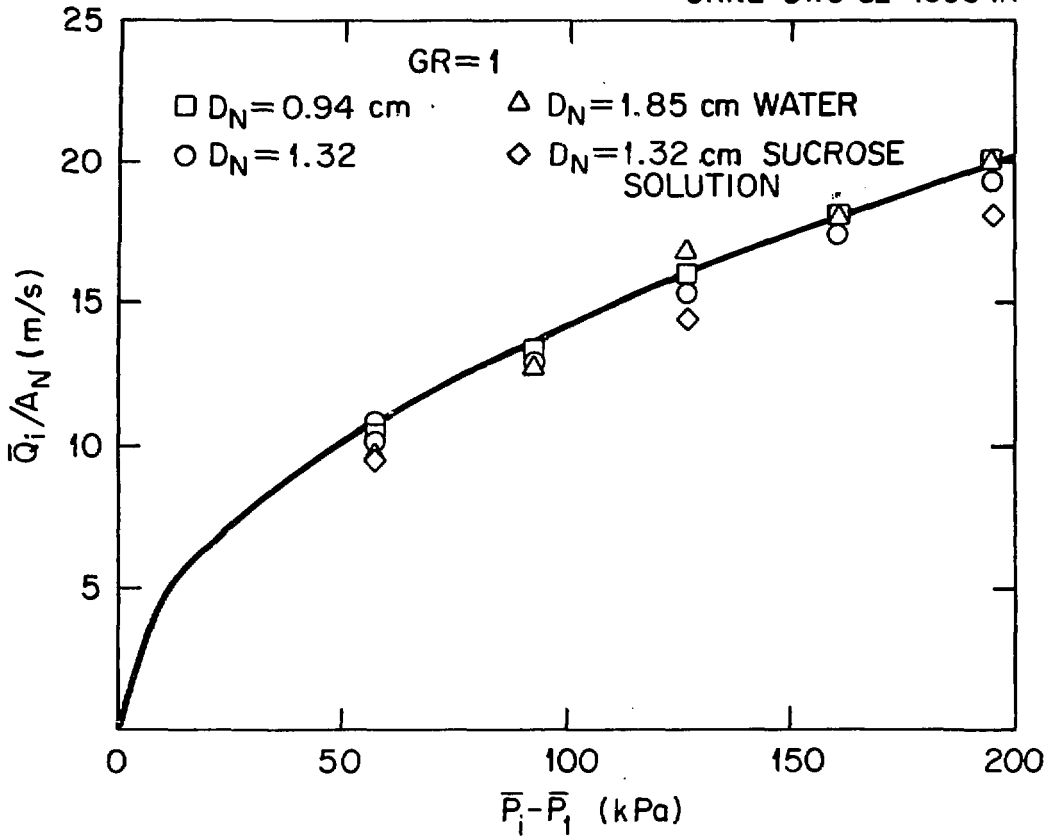


Fig. 3. The RFD throat velocities at varying input pressures for the three nozzle-diffuser combinations with a gap ratio of one.

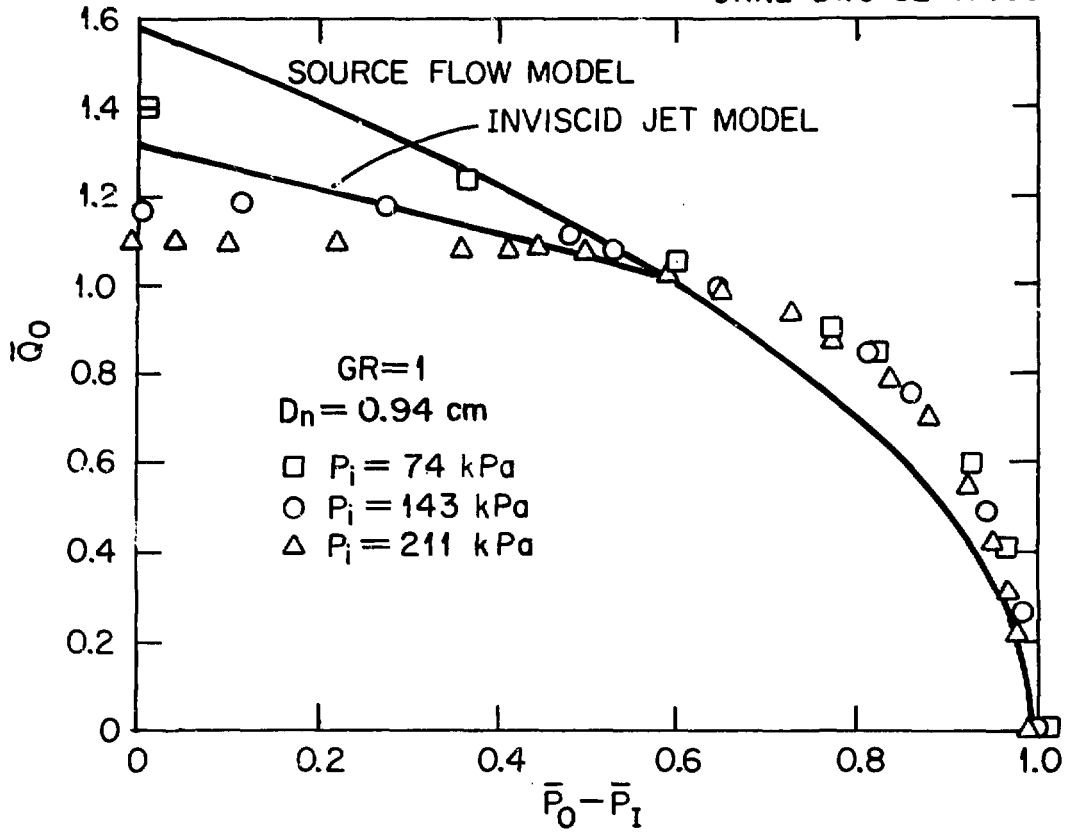


Fig. 4. Normalized output of an RFD with a throat diameter of 0.94 cm vs normalized output pressure at various input pressures.

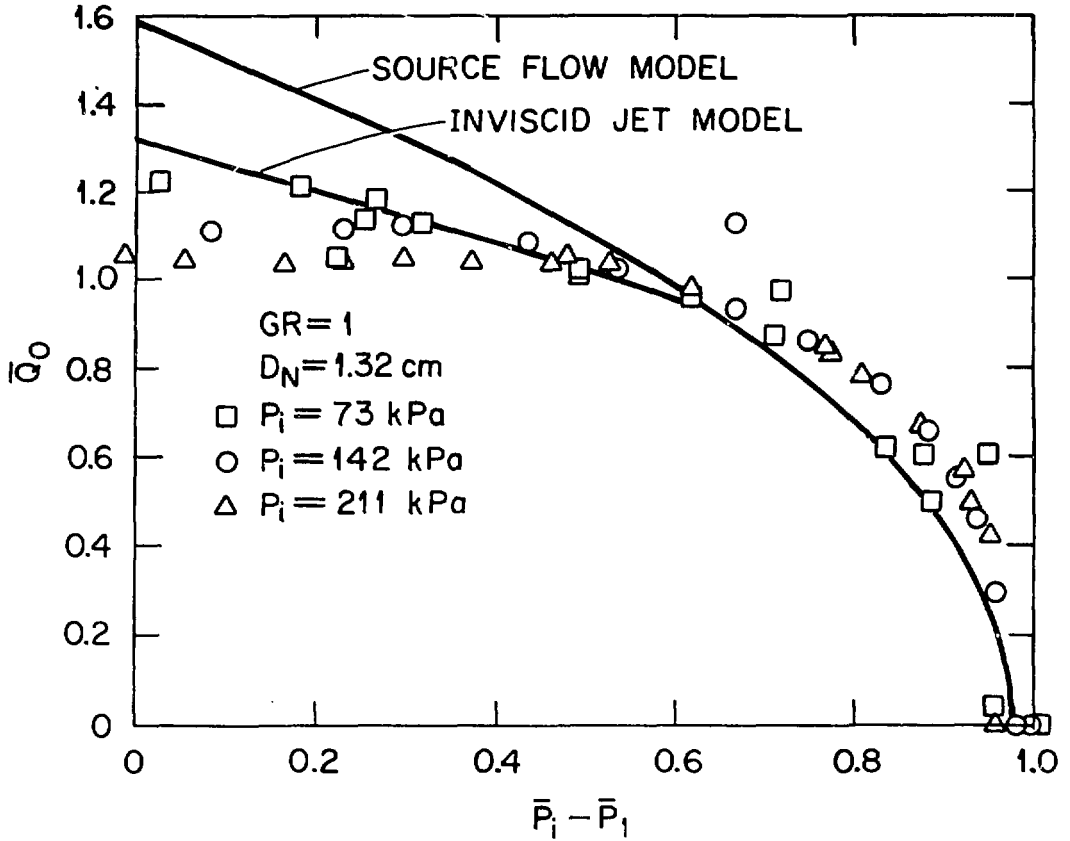


Fig. 5. Normalized output of an RFD with a throat diameter of 1.32 cm vs normalized output pressure at various input pressures.

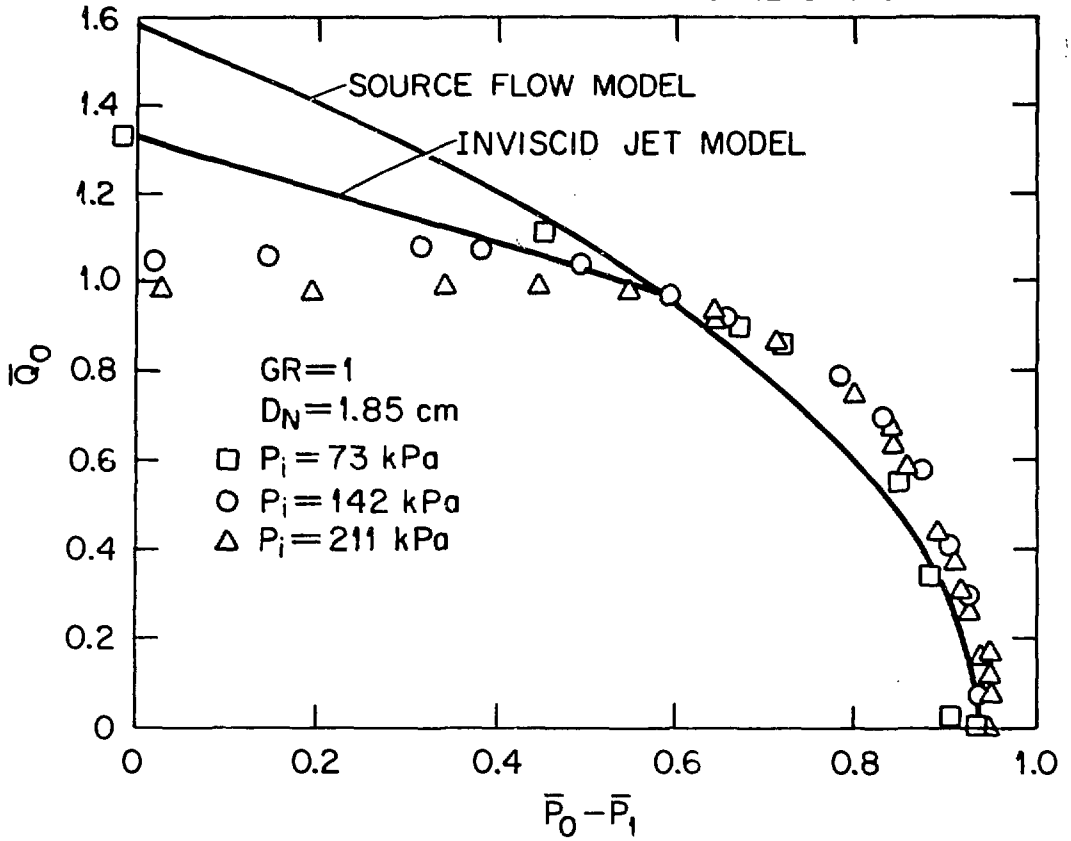


Fig. 6. Normalized output of an RFD with various gap ratios at a constant input pressure.

impedances. It is observed, however, that as the load impedance is decreased, the data tend to diverge with the lowest input pressure exhibiting a continued increase in output flow with a decrease in output pressure. The data for the two highest input pressures are observed to flatten out or saturate as the load impedance is reduced, with the highest supply pressure saturating first. As previously noted, the two models yield identical results for large load impedances but diverge as the load impedance is reduced. The inviscid jet model appears to predict the trend of the data reasonably accurately for the lowest input pressure for all three RFD sizes. The model does not, of course, explicitly predict the saturation of the output flow data.

The effect of fluid property variation on the output characteristics was tested using the 40 wt % sucrose solution with a density of 1170 kg/m^3 and kinematic viscosity of $6 \text{ m}^2/\text{s}$. These data are presented in Fig. 7 for the 1.32-cm nozzle along with the previously presented data for water for comparison purposes. Inspection of the data in this figure indicates no discernible or significant difference in the output characteristics due to this increase in viscosity and density.

The successful operation of the RFD dictates that the nozzle exit and receiver inlet be separated by a gap. To assess the effect of the size of the gap on the performance of the RFD, data were taken for gap ratios of 0.5, 1.0, and 1.5. A portion of this data is presented in Figs. 8 and 9 for supply pressures of 73 and 210 kPa respectively. Figure 9 indicates a slight performance dependency on the gap ratio, with the gap ratio of unity yielding slightly superior performance as

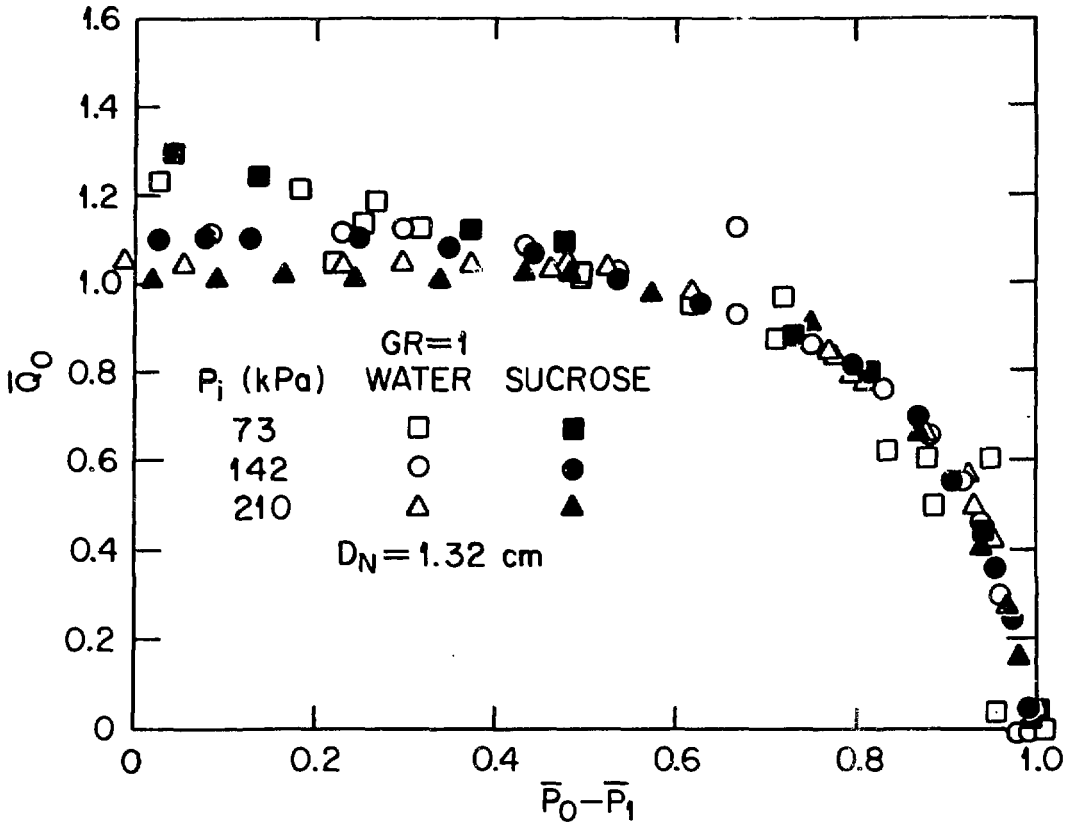


Fig. 7. Normalized output characteristics of an RFD with a throat diameter of 1.32 cm and a gap ratio of one, and various input pressures and aqueous solutions.

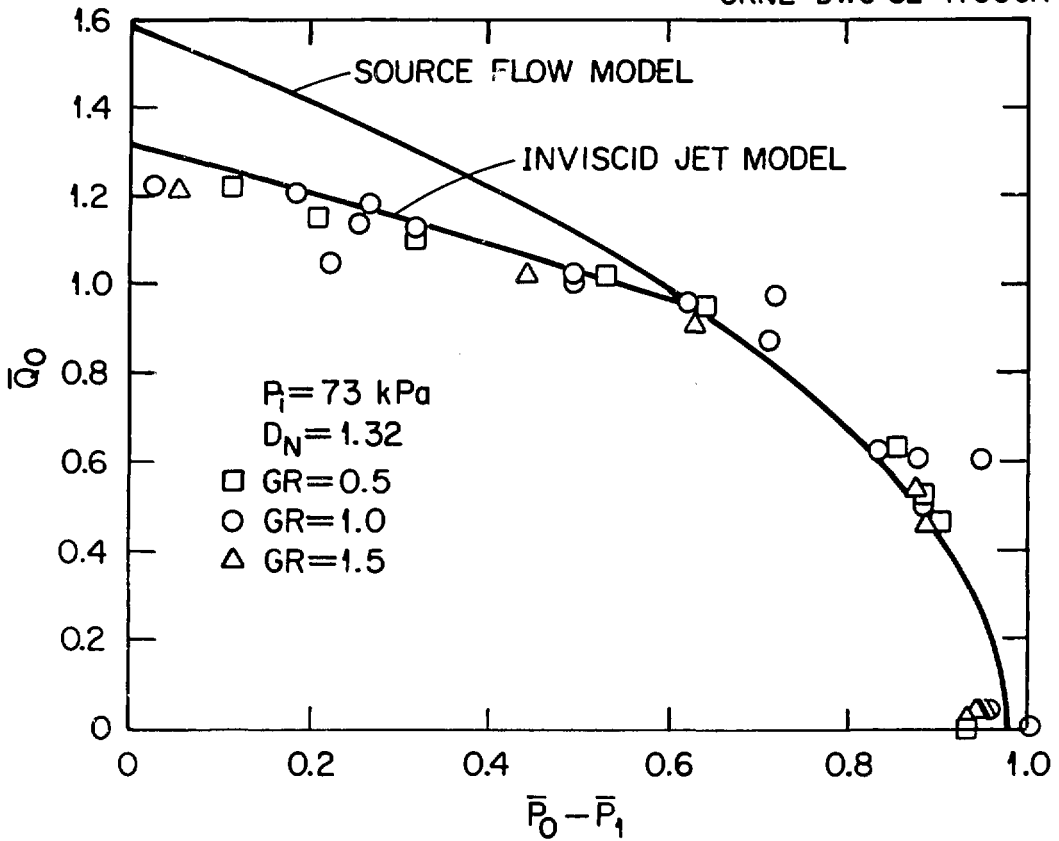


Fig. 8. Normalized output characteristics for an RFD with a throat diameter of 1.32 cm and an input pressure of 73 kPa at gap ratios of 0.5, 1.0, and 1.5.

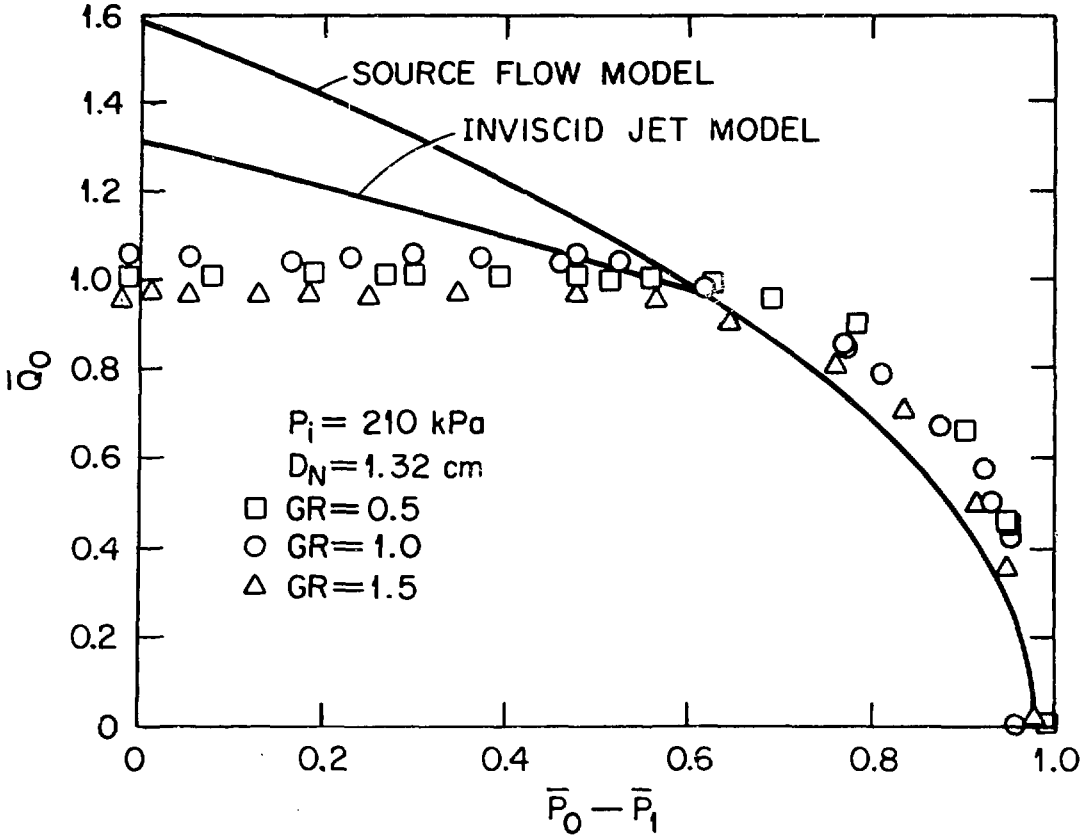


Fig. 9. Normalized output characteristics of an RFD with a throat diameter of 1.32 cm and input pressure of 210 kPa at gap ratios of 0.5, 1.0, and 1.5.

the load impedance is reduced. The data in Fig. 8 do not suggest any significant variation in the characteristics for the gap ratio range tested.

One disturbing aspect of the output characteristics of the RFD is the saturation of the output flow as the output pressure is reduced for supply pressures of 142 and 210 kPa. Since it has been shown¹¹ that the performance of a diffuser is highly dependent on the nature of the flow at the diffuser inlet, it was decided to determine whether or not "quieting" the flow entering the diffuser would yield improvements in the performance of the RFD as well as preventing possible premature separation. This was to be accomplished by a receiver/diffuser design with a constant area developing section preceding the diffuser in order to allow flow disturbances to decay before reaching the diffuser inlet. A portion of the data taken with the RFD having a developing section in the receiver/diffuser is presented in Figs. 10 and 11 for supply pressures of 73 and 210 kPa respectively. Also presented in these figures are data taken without the developing section for comparison purposes. It is evident from inspection of the data in these figures that any potential increase in performance due to flow disturbances being eliminated is more than offset by the increase in viscous losses in the developing section, yielding a slight decrease in overall performance. The saturation point of the flow in Fig. 11 is noted to be essentially unchanged.

The cause of the flow saturation in the receiver/diffuser is believed to be due to cavitation. Reid¹² has demonstrated that for a jet incident upon the receiver inlet of a receiver/diffuser, the pressure immediately inside the receiver entrance may be reduced

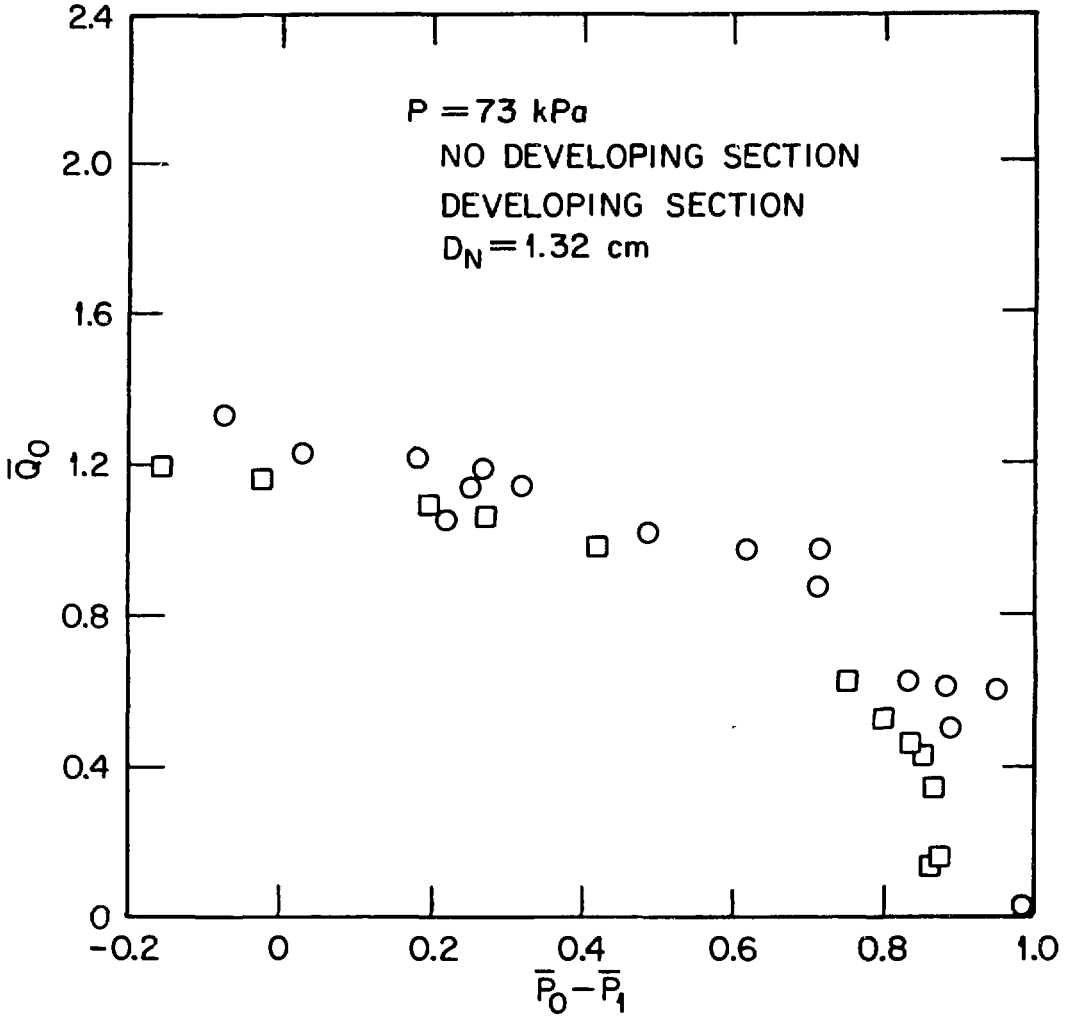


Fig. 10. Output characteristics for diffuser with developing section and $P_i = 73 \text{ kPa}$.

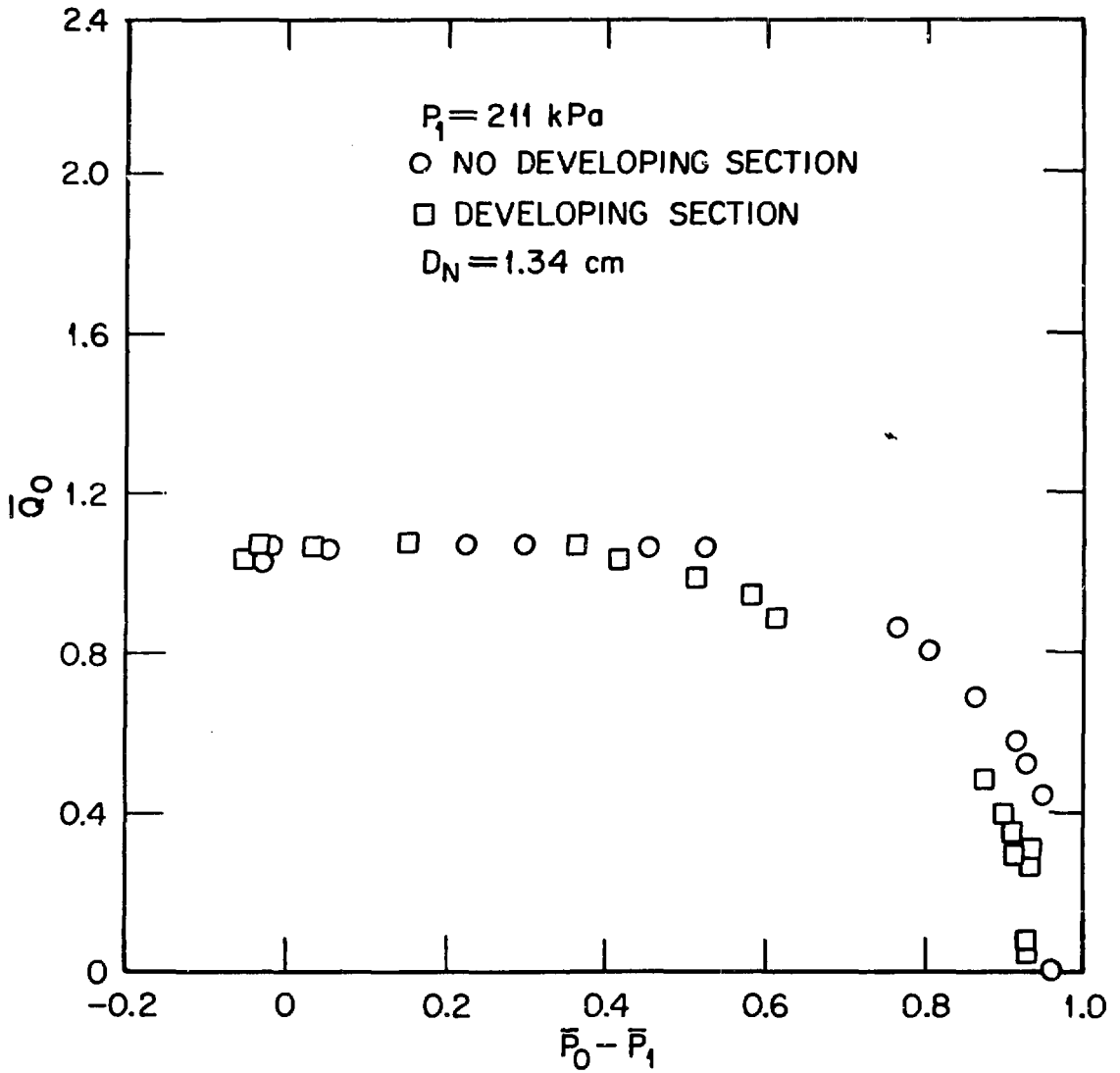


Fig. 11. Output characteristics for diffuser with developing section and $P_i = 211 \text{ kPa}$.

significantly below the ambient pressure as the load impedance is reduced. He did not encounter cavitation since air was utilized as his working fluid, but the normalized pressures he measured in the receiver were low enough to cause cavitation of most fluids, assuming dynamic similarity.

If the validity of the inviscid jet model is assumed, some interesting calculations may be made. Using a plenum pressure of 117 kPa, which is essentially equal to the experimental value, the pressure immediately inside the receiver inlet may be calculated from the model. These predicted pressures for supply pressures of 73, 142, and 211 kPa are presented in Fig. 12 as a function of the normalized static pressure rise across the receiver/diffuser. Although all pressures presented and discussed thus far have been gage pressures, it is noted that P_2 is presented in absolute units.

Inspection of Fig. 12 indicates that for all supply pressures, the receiver inlet pressure decreases as the load impedance is reduced. The two highest supply pressures yield receiver inlet pressures in the negative absolute pressure region, which is, of course, impossible. This suggests that the pressure in the receiver inlet will eventually be reduced to a point as the load impedance is reduced where cavitation will occur. This cavitation pressure point is dependent on the temperature of the fluid as well as the dissolved gases in the fluid. It is observed that the lowest supply pressure does not yield pressure predictions low enough to expect cavitation to occur as the experimental data suggests.

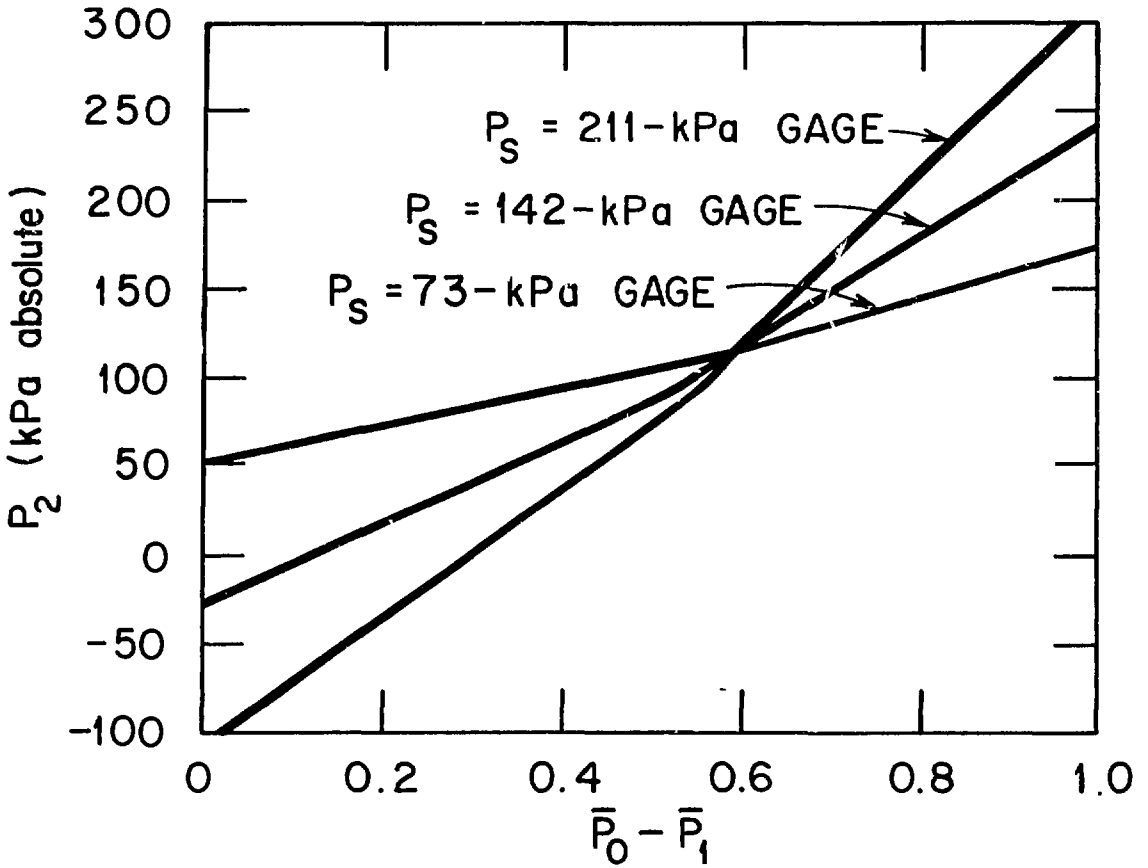


Fig. 12. Predicted receiver entrance pressure.

4. CONCLUSIONS

The experimental performance characteristics of axisymmetric RFDs presented herein are observed to agree with the mathematical model predictions for the lowest supply pressure tested. The output pressure-flow data are characterized by the output volumetric flow rate saturating as the load impedance is reduced for the two highest supply pressures. This flow saturation is likely due to cavitation of the flow in the inlet region of the receiver caused by large curvilinear velocity gradients in the receiver/diffuser. Within the range of variables tested, the normalized performance of the RFD is a weak function of the size of the RFD, the axial gap separating the nozzle exit from the receiver inlet, and the density and viscosity of the fluid.

REFERENCES

1. J. H. Mammon, "Fluidics Score in Quest for CPI Applications," Chem. Eng. 33-37 (July 1980).
2. J. C. Campbell and R. F. Jackson, "Review of Remote Handling Experience and Philosophy in a Reprocessing Plant in the United Kingdom," pp. 186-205 in Proc. 25th Conf. Remote Systems Technology, American Nuclear Society, San Francisco, CA (1977).
3. J. P. Baker, "A Comparison of Fluidic Diodes," Second Cranfield Fluidics Conf., Cambridge, England, D6-(88-115), January 1967.
4. B. E. A. Jacobs, "Fluidic Diodes," pp. 11-19 in Proc. of the Symposium for Process Control, University of Surrey, Gilford, England, 1973.
5. J. R. Tippetts, "A Fluidic Pump for Use in Nuclear Fuel Reprocessing," Proc. 5th International Fluid Power Symposium, University of Durham, England, 1978.
6. J. R. Tippetts, "Some Recent Developments in Fluidic Pumping," Proc. of Pumps 1979, 6th Tech. Conf. British Manufacturers Association, Canterbury, England, 1979.
7. J. R. Tippetts, G. H. Priestman, and D. Thompson, "Developments in Power Fluidics for Application in Nuclear Plant," Trans. ASME 103 1981.
8. G. V. Smith and R. M. Counce, "Performance Characteristics of a Plane Wall Venturi-Like Reverse Flow Diverter," Ind. Eng. Chem. Process Des. Dev. 23 (1984).
9. R. W. Box and S. J. Kline, J. Basic Eng. 84, 303-12 (1962).
10. J. M. Kirshner, Jet Dynamics and its Applications to the Beam Deflection Amplifier, HDL-TR-1630, Harry Diamond Laboratories, July 1973.
11. P. W. Runstadler, Jr., F. X. Dolan, and R. C. Dean, Jr., Diffuser Data Book, TN-186, Creare Technical Information Service, Hanover, NJ. 1975.
12. K. N. Reid, Static and Dynamic Interaction of a Fluid Jet and a Receiver/Diffuser, ScD thesis, Department of Mechanical Engineering, Massachusetts Institute of Technology, 1964.

Nomenclature

Variables

A	Area
C_d	Discharge coefficient
C_p	Pressure recovery coefficient
D	Diameter
GR	Gap ratio, nozzle-receiver separation distance divided by diameter of nozzle
K_d	Diffuser loss coefficient
P	Pressure
Q	Volumetric flow rate
v	Velocity
ρ	Density

Subscripts

i	Input
in	Induced flow
j	Jet flow
n	Nozzle outlet
o	Diffuser outlet
r	Receiver inlet
s	Source
1	Region between nozzle and receiver
2	Receiver inlet section
3	Receiver exit, diffuser inlet

Superscripts

— Bar atop variable indicates normalized quantity